REVIEW ARTICLE

Recent advances in synthesis, structural properties, and regulation of nickel sulfide-based heterostructures for environmental water remediation: an insight review

Anuradha Sharma[1] · Peter R. Makgwane[2,3] · Eric Lichtfouse[4] · Naveen Kumar[1] · Ahmad Hosseini Bandegharaei[5] · Muhammad Tahir[6]

Abstract

Heterostructured nanomaterials exhibit pronounced potential in environmental science, including the water purification, pollutant monitoring, and environmental remediation. Especially, their application through advanced oxidation processes has been found capable and adaptable in waste water treatment. In semiconductor photocatalysts, metal sulfides are the leading materials. However, for further modifications, the progresses on specific materials need to be overviewed. Among metal sulfides, nickel sulfides are the emerging semiconductors due to relatively narrow band gaps, high thermal and chemical stability, and cost effectiveness. The aim of the present review is to conduct a thorough analysis and summary of recent progress in the application of nickel sulfide-based heterostructures in water decontamination. Initially, the review introduces the emerging needs of the materials for environment following the characteristics features of metal sulfides with emphasis on nickel sulfides. Subsequently, synthesis strategies and structural properties of nickel sulfide (NiS and NiS_2)-based photocatalysts are discussed. Herein, controlled synthesis procedures to influence their active structure, compositions, shape, and size for the enhanced photocatalytic performances are also considered. Furthermore, there is discussion on heterostructures formed by metal modification, metal oxides, and carbon hybridized nanocomposites. In the continuation, the modified characteristics are investigated which favors the photocatalytic processes for degradation of organic contaminations in water. The overall study highlights significant improvements in degradation efficiency of hetero-interfaced NiS and NiS_2 photocatalysts towards organics that are comparable to expensive noble-metal photocatalysts. Finally, we also added a little on prospects for future advancement of nickel sulfide-based photocatalysts for applications in sustainable environmental remediation.

Introduction

The accelerated rates of industrialization all over the world and over population are the two major sources of several kinds of contaminants in water that are deteriorating the environment (Kummu et al. 2016; Lichtfouse et al. 2021; Izzudin et al. 2021). As per European Community (EC) and the United States Environmental Protection Agency (USEPA), organic pollutants include different halogenated pesticides, fertilizers, and biphenyls, monocyclic and polynuclear aliphatic or aromatic compounds, halogenated ethers, and phthalate acid esters along with some miscellaneous compounds (Wild and Jones 1991). In the contaminated wastewater treatment, some suitable methods are adsorption, membrane technologies, coagulation, and photocatalytic degradation (Kumar et al. 2019b; Akshatha et al. 2020; Alrobei et al. 2021). In this regard, photocatalysis has been intensely researched and widely applied in several areas including solar energy utilization, water splitting, medical and health care, pollutant degradation, and environmental governance (Anwer et al. 2019). This technology is driven by solar energy wherein simple operation, mild reaction conditions, and producing no secondary pollution make it

---

Responsible Editor: George Z. Kyzas

✉ Naveen Kumar
naveenkumar.chem@mdurohtak.ac.in

Extended author information available on the last page of the article

an effective strategy to solve global problems (Meng et al. 2019; Dhiman et al. 2022).

The photocatalysis process is a sort of advanced oxidative processes where a semiconductor material absorbs light of energy equal to or greater than its band gap energy, leading excitations of electrons from valence band to the conduction band (Soltani et al. 2012; Sharma et al. 2022). The generated electron–hole (e^-/h^+) pairs further produce different free radicals like hydroxyl, superoxide anion radicals in the reaction system to redox to activate the adsorbed compounds on the surface of the photocatalyst (Sharma et al. 2021b). Thus, photo-induced degradation of the organic compounds with the help of photo-chemically active semiconductor materials is one of the most interesting topics of environmental and global management (Adhikari et al. 2013). Therefore, the development of photocatalysts is the efficient strategy to overcome the issues of industrial wastewater remediation and energy crisis (Kumar et al. 2019a; Gan et al. 2021).

In advanced oxidation process, the frequently reported materials are transition metal oxides (Okpara et al. 2023), nitrides (Luo et al. 2023), carbides (Mabuea et al. 2022), phosphides (Han et al. 2021), sulfides (Wu et al. 2022), and selenides (Nawaz et al. 2023). Especially, the metal sulfides have emerged as promising candidates for water purification-relevant applications. In the metal sulfides, MoS_2, CdS, SnS, and NiS are the frequently studied ones (Mishra and Chun 2015; Ong et al. 2016; Li et al. 2018; Wang et al. 2018; Mittal et al. 2019; Sharma et al. 2021a; Kumari et al. 2021; Passi and Pal 2021). Among the metal sulfides, nickel sulfides have attracted the attention due to ease of fabrication, low cost, and low toxicity and have widespread applications in environmental science (Wang et al. 2007).

These metal sulfides due to their narrow band gaps have capability to absorb in visible light regions and therefore have applied in the photocatalytic reactions extensively (Lopes et al. 2021). Further, the heterostructure interfaces of nickel sulfides with different materials like metal oxides, sulfides, and carbon-based structures improves the photocatalytic activity performances (Zhang et al. 2012; Wang et al. 2018; Zhao et al. 2019). Nickel sulfides exhibit low band gap value compared to tradition semiconductors such as TiO_2, ZnO, SnO_2, and CeO_2 (Rajamanickam et al. 2015). A properly matched p–n junction formation can significantly induce electric field at the interfaces, which in turn expands spectral response range and efficient generation, separation, and transference of the photoexcited charge carriers (Qian et al. 2018). However, there are a number of articles published on transition metal-based catalysts, but the main focus lies on electrochemical energy storage and photocatalysis with an emphasize on the catalyst synthesis methods, characterization techniques, morphology, and structure control. Despite the progress in heterogeneous catalysis for water purification, specially the study on nickel metal sulfide-based photocatalysis is still in its infancy, and the application in heterogeneous catalysis to treat contaminated water has never been reviewed till now.

The present review article emphasized on synthesis strategies and developments in characteristic properties for nickel sulfide and the assisted materials. In the modification pathways, special attention has been given on the heterostructures with metals, metal oxides, metal sulfides, and different carbon-based materials (Fig. 1). Finally, the nickel sulfide heterostructured materials are discussed scientifically for the photocatalytic applications towards decontamination of various organic pollutants for environmental remediation.

Properties of NiS and NiS$_2$ semiconductors

Transition metal sulfides have been reported to exhibit diverse stoichiometries compositions and structure morphologies. This is ascribed to the hybridizing of 3 s and 3p orbitals with the 3d orbitals that stabilize adjacent six cations and arranged in a trigonal–pyramidal configuration. The S–S bonds resulting in molecular anions and large dipole moments of the anions support the formation of layered structures (Rao and Pisharody 1976). In this regard, nickel sulfides reported generally in literature with the stoichiometries Ni_3S_2, Ni_3S_4, NiS, Ni_7S_6, Ni_9S_8, NiS_2, α-NiS, β-NiS, α/β-NiS composite, and structures of mixed phases with the

Fig. 1 A general layout of nickel sulfide heterostructures, properties, and synthesis strategies
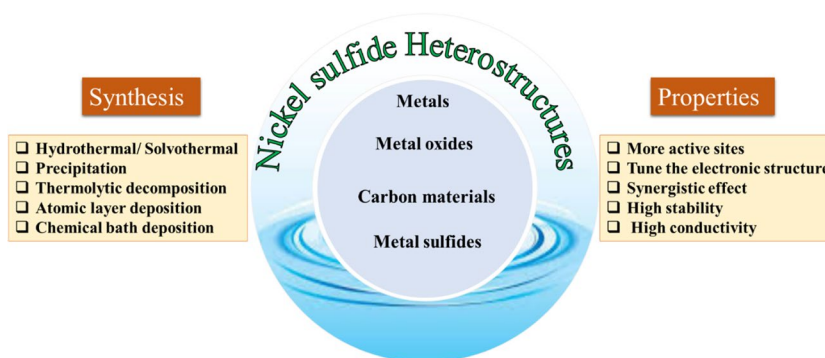
films and nanosheets, nanospheres, nanotubes, nanorods, nanowires, and nanoplate-like (Dong et al. 2011; Zhou et al. 2013; Li et al. 2014, 2020; Tang et al. 2015; Shi et al. 2019; Shombe et al. 2020). Among the variety of nickel sulfide phases, most of the phases are found at lower temperatures. Out of the different nickel sulfide phases, two important ones are (i) low-temperature rhombohedral phase β-NiS and (ii) high-temperature hexagonal α-NiS phase. Each phase of nickel sulfide has its own physical and chemical properties and is useful when applied in particular field (Zheng et al. 2019). The synthesis of nickel sulfide nanocrystals with particular structural features for specific applications is very challenging. However, synthesis of phase selective materials enables the researchers to investigate the phase-dependent properties and extend the applicability of the respective materials and also provides new paths to design novel highly photoactive nanomaterials (Lim et al. 2006). It is well-known that the composition, phase, morphology, and size of any material are largely decided by the fabrication reaction kinetics and the related thermodynamics (Huang et al. 2015). Therefore, the structural characteristics of the synthesized material are probably altered by the control of experimental conditions. In addition, to synthesize nickel sulfide with specific structure and phase, understanding of the influencing factors for the crystal formation is necessary. The most important differences among the various classes of nickel sulfides are the stoichiometric ratios of nickel and sulfur and the different oxidation states of sulfur and nickel (S^{2-}, S_2^{2-}, Ni^{2+}, and Ni^{3+}) (Rhodes et al. 2017). It is documented that there are several factors which effect the composition and phase of the synthesized nickel sulfides (Manjunatha et al. 2020). The reactivity and concentration of the used precursors, solvent and its pH, reaction temperature, sources of nickel and sulfur, organic ligands, and reaction rate are the main decisive factors for the phase selective preparation of nickel sulfide materials (Hu et al. 2022a).

The fractal geometry-nickel sulfide dendritic structures were developed via chemical vapor deposition method (Shriber et al. 2022), and the growth mechanism of the crystals was examined. Different compositions were found during the nucleation including various stoichiometries of $Ni_{0.96}S$ (hexagonal phase), $Ni_{0.99}S$ (hexagonal phase), Ni_XS_6 (monoclinic phase), $(Ni_7S_6)_{3.25}$ (orthorhombic phase), and, finally, the Ni_3S_2 in rhombohedral phase were identified. The α-NiS is reported as the metastable phase at ambient conditions and gets transformed into the more stable β-NiS phase at lower temperatures exhibiting rhombohedral structure (Yousfi et al. 2010). Investigations of transformation mechanisms revealed that change in temperature and the sulfur content in the α- NiS significantly changes the structural transformation route. Also, the structural properties of nickel sulfide are determined by the source of sulfur taken in the reaction. Cubic polydymite (Ni_3S_4) were obtained (Balayeva

et al. 2017) when Na_2S was used as the source of sulfur (S), exploiting 0.5 M of nickel precursor in 24 h reaction time. On the other hand, when thiourea was used as S-resource, rhombohedral NiS nanocrystals were fabricated. A phase transition–orthorhombic Ni_7S_6 nanocrystals were observed when vacuum annealing was done for 8 h at 180 °C.

The structural composition can be varied by altering the atomic ratios of the precursors used for Ni and S respectively. For example, when various 2:1, 3:1, 1:2, and 1:3 atomic ratios of Ni and S were used to synthesize nickel sulfides (Khan et al. 2021), the corresponding crystal structure and phases were verified in the XRD patterns as shown in Fig. 2a. The fabricated samples were indexed to diffraction peaks at (002), (102), (101), (200), (110), (201), and (112) planes which supported the formation of NiS nanocrystals phase. Another work investigated the effect of reaction temperature on the phase compositions and reported that sulfur-rich nickel sulfides are obtained at higher temperatures (Gou et al. 2017). At 160 °C, the diffraction peaks were ascribed to the pure NiS rhombohedral phase, while mixed phases of cubic Ni_3S_4 and rhombohedral NiS were obtained at 180 and 200 °C, respectively (Fig. 2b).

Regulation of reactivity of precursors and ratio of metal ions to the sulfur source is also an important parameter. Sulfur-rich phases were obtained when weaker C─S bonds were present in the sulfur source (Rhodes et al. 2017), due to which more active sulfur species are released to react with metal ions and produce sulfur-rich sulfide product. In addition to it, there are some strategies which focus on the production of sulfur-deficient nickel sulfides. For instance, variation in the amount of coordination agent (Hu et al. 2022b) transformed the β-NiS/α-NiS/Ni_3S_4 composition to β-NiS/α-NiS and finally to pure β-NiS. Another work (Hu et al. 2022a) reported the effect of solvent pH and found lower pH values suitable for S-rich sulfides. When 1 M HCl was used as the solvent, bulk structured pure NiS_2 phase was obtained, while layered structures of β-NiS were obtained with 2 M KOH solution as the solvent. Such types of observations are also supported with the DFT analysis. In acidic conditions, S atoms become more competitive for the Ni atoms as compared to the alkaline medium since the distance between the associated atoms is lesser, and the involved atoms can approach more easily. Moreover, the content of sulfur to nickel influences the association of the different atoms and, hence, the bond length between the atoms (Hu et al. 2022a). Therefore, the morphology and the respective structures are also altered. Figure 2c shows the correlation between the S -content and Ni-S bond distance and the obtained structures. The rate of feeding the starting materials during the synthesis introduces in homogeneity into the material. In a report, the effect of different feeding rates of the precursors was explained (Chandra Patel et al. 2021). It was observed that NiS_2 is favored only at low feeding rates since relative
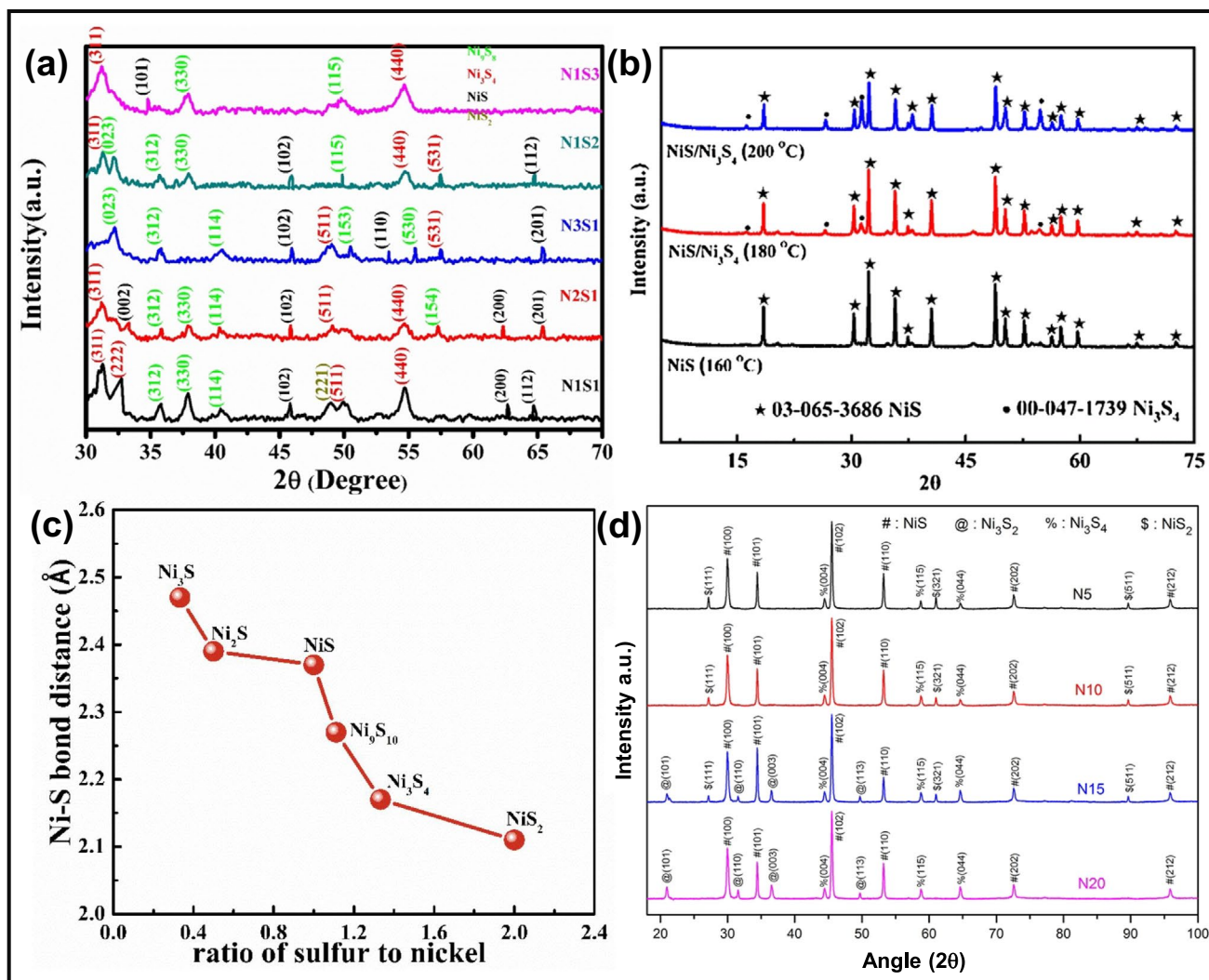
Fig. 2 **a** XRD spectra of the synthesize nickel sulfides at different atomic ratios of Ni and S (1:1, 2:1, 3:1, 1:2, and 1:3). Reprinted with permission from ref. (Khan et al. 2021). Copyright 2021 Elsevier. **b** Effect of temperature (160, 180, and 200 °C) on the different phase ratios of nickel sulfides. Reprinted with permission from ref. (Gou et al. 2017). Copyright 2017 Elsevier. **c** Correlation of the S- content and Ni-S bond distance obtained from (Materials Project (https://materialsproject.org/)). Reprinted with permission from ref. (Hu et al. 2022a). Copyright 2022 Elsevier. **d** Effect of feeding rates of the Ni and S precursors on the existence of nickel sulfide phases. Reprinted with permission from ref. (Chandra Patel et al. 2021). Copyright 2021 Elsevier

amount of the NiS_2 phase goes on decreasing with increase in the flow rates from 5 to 15 ml/min and becomes absent at 20 ml/min flow rate (Fig. 2d). On the other hand, at the flow rate of 10 ml/min, maximum content of α-NiS was obtained. Thus, it is concluded that the rate of adding the precursors greatly affects the existence of phases in nickel sulfides.

Nickel sulfide composites with other metal sulfides have been reported that successfully form heterojunctions of the two materials and allow sufficient band offset for electron–hole separation (Zhao et al. 2022; Yendrapati et al. 2022). ZnS/Ni_xS_y heterojunctions were obtained via one-pot synthesis and exhibited proper band alignment (Khan et al. 2020). The band structures and electron density of

states for NiS and NiS_2 were investigated with the theoretical DFT study as shown in Fig. 3a–e. Using the calculated positions for NiS and NiS_2 Fermi levels as well as a Schottky-type junction with downward band bending was generated (Fig. 3e).

Synthesis strategies of nickel sulfide-based photocatalysts

The nickel sulfide network is highly interesting owing to the numerous phases that it exhibits; including $β-Ni_3S_2$, Ni_3S_4, α- $Ni_{3+x}S_2$, Ni_4S_{3+x}, Ni_9S_8, Ni_7S_6, Ni_6S_5, NiS_2, and α-NiS,
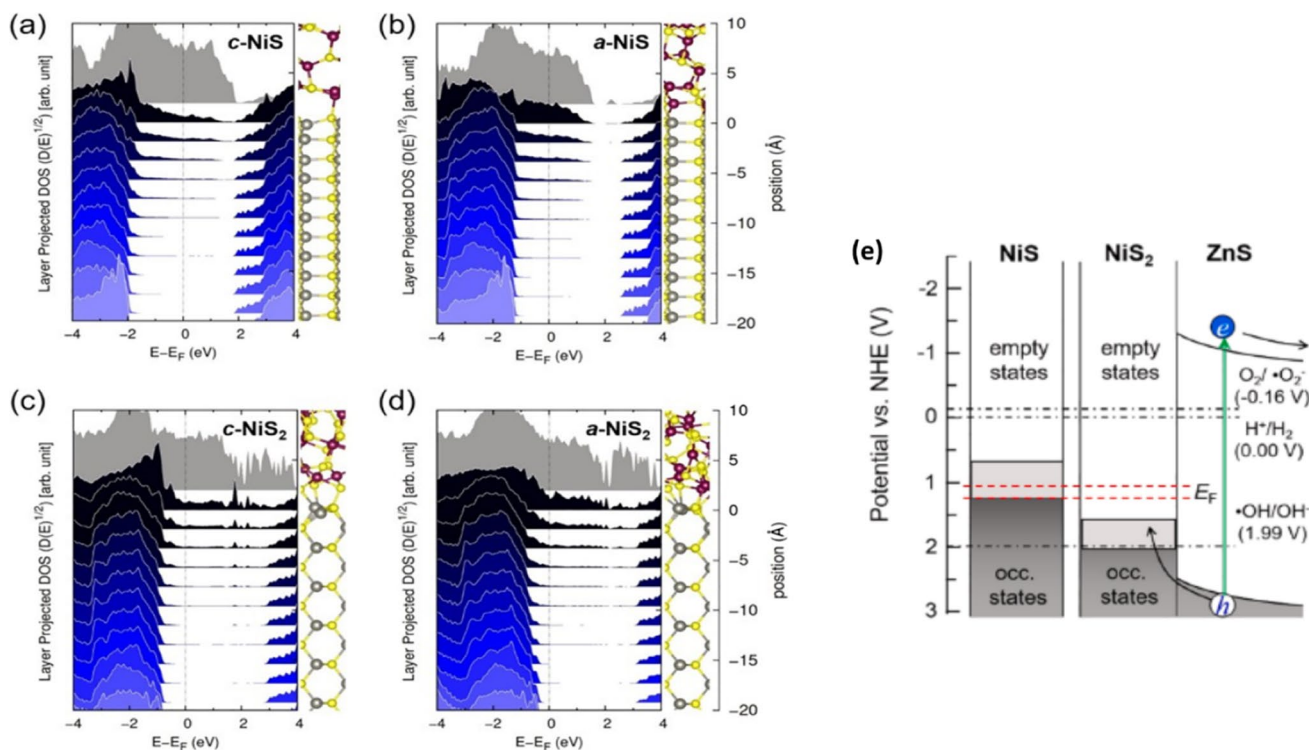
Fig. 3 Electron density of states (DOS) projected onto each layer of **a** c-NiS, **b** a-NiS **c** c-NiS₂, and **d** a-NiS₂ with a c-ZnS (1 1 0) surface. Note that VBMs of ZnS locate at **a** 1.80, **b** 1.27 eV, **c** 0.91, and **d** 0.50 eV below the Fermi level. **e** Band diagram drawn using the valence band level of ZnS relative to Fermi level from DFT simulations and measured band edges of NiS. Reprinted with permission from ref. (Khan et al. 2020). Copyright 2020 Elsevier

β- NiS (Emadi et al. 2017). Since, in the present article, we are dealing especially with NiS and NiS₂, various synthesis methods and the resulting morphologies are listed in Table 1. The constituent elements itself declare that the preparation of nickel sulfide materials are affected by Ni precursor and sulfur source than the conditions being used in their respective synthesis procedures. The most prominent nickel salts that are used in the preparations of NiS or NiS₂ are nickel (II) nitrate, nickel (II) chloride, and nickel (II) acetate tetrahydrate. For sulfur source, the widely used are ammonium sulfide, sodium sulfide, and thiourea. Other important matter of synthesis is the procedure or method adopted to get the desired Ni sulfide.

NiS-based photocatalysts

NiS is reported to possess two phases: (i) hexagonal and (ii) rhombohedral phase (Sun 2003; Ghezelbash et al. 2004). The synthesized phase and the corresponding morphology of sample are largely determined by the precursor used, reaction route, or method selected along with the synthesis conditions employed. For example, NiS with β-phase and nanoflakes morphology was obtained (Zhao et al. 2009) when reaction was carried out for 12 h, while NPs morphology instead of nanoflakes were obtained for the reaction time of up to 3 h. Pristine NiS can be prepared via solvothermal approach using nickel nitrate as Ni source and thiourea (CH₄N₂S) as the sulfur source in ethylene glycol solvent. Literature reveals that during the synthesis of nickel sulfides, obtaining single phase of either β-NiS or α-NiS is difficult task. Generally, the formation of mixed phases is obtained in case of NiS. Up to date various synthesis methods have been utilized to prepare controlled phases of nickel sulfides including solvothermal, microwave, and hot injection method (Idris et al. 2011; Yang et al. 2014; Karthikeyan et al. 2015). NiS preparation using square planar nickel bis (dithiocarbonate) complexes [Ni(S₂CNR₂)₂] exhibited α-NiS to β-NiS with phase transformation at high temperature of 280 °C (Roffey et al. 2016). Band gaps for NiS can be tuned by adjusting the temperature and changing capping agents such as citric acid, polyvinylpyrrolidone, and β-cyclodextrin (Molla et al. 2016). Similarly, another study reported α and β phases of NiS synthesized by green synthesis protocol using water and ethanol under solvothermal conditions (Muniyappa et al. 2022). When the precursors of (Ni (CH₃COO)₂·4H₂O, (NH₂)₂CS, and NaC₁₂H₅5SO₄) were dissolved in pure ethanol, α-NiS was obtained whereas β-NiS phase was observed with 1:2 ratio of ethanol to water.

Table 1 Synthesis method, morphology, and precursors used for the preparation of nickel sulfides and their heterostructures

Catalyst	Nickel precursor	Sulfur source	Synthesis method	Morphology	Reference
NiS	$Ni(NO_3)_2 \cdot xH_2O$	$C_{12}H_{25}SH$	Thermolytic decomposition (190 °C, 5 h)	Nanorods	(Ghezelbash et al. 2004)
NiS and NiS_2	$Ni(NO_3)_3$	$Na_2S_2O_3$	Hydrothermal (180 °C, 12 h)	Hollow microspheres	(Luo et al. 2017)
α/β-NiS	$Ni(CH_3COO)_2 \cdot 4H_2O$	Thiourea	Solvothermal (200 °C, 8 h)	Elongated oval-shaped particles	(Muniyappa et al. 2022)
$CuS-NiS-TiO_2$	$Ni(NO_3)_2 \cdot 6H_2O$	Thiourea	Hydrothermal (160 °C, 12 h)	Microspheres	(Wang et al. 2014)
$ZnO/NiS@NiO/rGO$	$Ni(CH_3COO)_2 \cdot 4H_2O$	CH_4N_2S	Solvothermal (150 °C, 4 h)	Nanoparticles	(Liu and Li 2021)
NiS/rGO	$NiCl_2 \cdot 6H_2O$	Na_2S	Hydrothermal (170 °C, 5 h)	Nanoparticles	(Arumugam et al. 2020)
$Ni(OH)_2/NiS_x/BiVO_4$	$Ni(NO_3)_3$	Na_2S	Precipitation (-)	Nanoparticles	(Huang et al. 2022)
NiS/CdS	$Ni(NO_3)_2 \cdot 6H_2O$	Thiourea	Solvothermal (150 °C, 12 h)	Nanoparticles and flower	(Liu et al. 2021)
AC-NiS/CoS	$NiCl_2 \cdot 6H_2O$	Na_2S	Precipitation (-)	Spherical-nanosheets	(Artagan et al. 2021)
$NiS_2/g-C_3N_4$	$NiCl_2 \cdot 6H_2O$	Thiourea	Hydrothermal (120 °C, 24 h)	Nanosheet dispersed quantum dots	(Qin et al. 2020)
β-NiS/ $ZnIn_2S_4$	$NiC_4H_6O_4 \cdot 4H_2O$	Thiourea	Solvothermal (180 °C, 4 h)	Nanosheets	(Ding et al. 2021)
NiS/NU-1000 (MOF)	Bis(N,N′-ditert-butylacetamidinato) nickel(II)	nickel(II) sulfide	Atomic layer deposition (120 °C, 5 min)	–	(Peters et al. 2016)
$NiS-CuO@ ZnFe_2O_4$	$Ni(NO_3)_2 \cdot 2H_2O$	Na_2S	Chemical bath deposition (-)	Nanoarrays	(Chen et al. 2020b)
$CoNiS_x-C_3N_4$	$Ni(NO_3)_2 \cdot 6H_2O$	Thiourea	Thermal polymerization and Hydrothermal (120 °C, 5 h)	Polyhedrons and nano-particles	(Jiang et al. 2019)
$NiS/CuInS_2/NiO$	$Ni(CH_3COO)_2 \cdot 4H_2O$	C_2H_5NS	Successive ionic layer adsorption and reaction (25 °C)	Nanosheets	(Liu and Zhou 2020)
$Ni_3S_2-NiS_2-g-C_3N_4$	$Ni(OAc)_2$	CH_3CSNH_2	Hydrothermal (130 °C, 12 h)	Particles distributed over C_3N_4	(Xi et al. 2022)

A solvothermal technique is well known to achieve the nanostructures of different dimensions with controlled morphologies. Recently, multicomponent sulfides materials are receiving tremendous attention owing to their excellent optical properties and adjustable band gaps (Su et al. 2019). A one-pot solvothermal method was used to synthesize NiS/$Mn_{0.3}Cd_{0.7}S$ with p–n heterojunctions (Han et al. 2020). The NiS nanoclusters were highly dispersed onto surface of $Mn_{0.3}Cd_{0.7}S$ nanorods. Heterostructured composites of NiS with metal organic framework (MOF) have been prepared by the deposition of NiS on NU-1000, Zr (IV)-based MOF scaffold with the bis (N, N′-di-tert-butylacetamidinato) nickel- (II) and H_2S as the nickel and sulfur sources, respectively (Peters et al. 2016). A unique, one step method is reported in which MOF based on MIL-101 (Fe/Ni) was used as metallic source and calcined in the presence of Na_2S to prepare the NiS/γ-Fe_2O_3/C type-II heterojunction (Rashid et al. 2021). The MIL-101 (Fe/Ni) was used as a sacrificial template. Loading NiS on graphite-like carbon nitride (g-C_3N_4) nanosheets is also an effective strategy to prepare NiS heterojunctions. This can be achieved either directly loading or some intermediaries. The strategy using intermediary compounds has advantages over direct loading method involving (i) more efficient contact is possible between NiS and C_3N_4 nanosheets and (ii) proper orientation of the co-catalyst takes place due to the introduction of intermediaries. This reason may be the proper d-spacings existing in the intermediary material corresponding to both the species going to form heterojunctions. $CuWO_4$ was used as the intermediaries to prepare NiS/g-C_3N_4 photocatalyst (g-C_3N_4/NiS-W) (Xue et al. 2021). The overall synthesis procedure followed is depicted in Fig. 4a with the help of a schematic diagram. Moreover, carbon nanotubes (CNTs) consisting of cylindrical tubes are also considered as potential materials in forming nickel sulfide heterojunctions and utilized in several fields (Wang et al. 2019). Apart from these, MoS_2 is
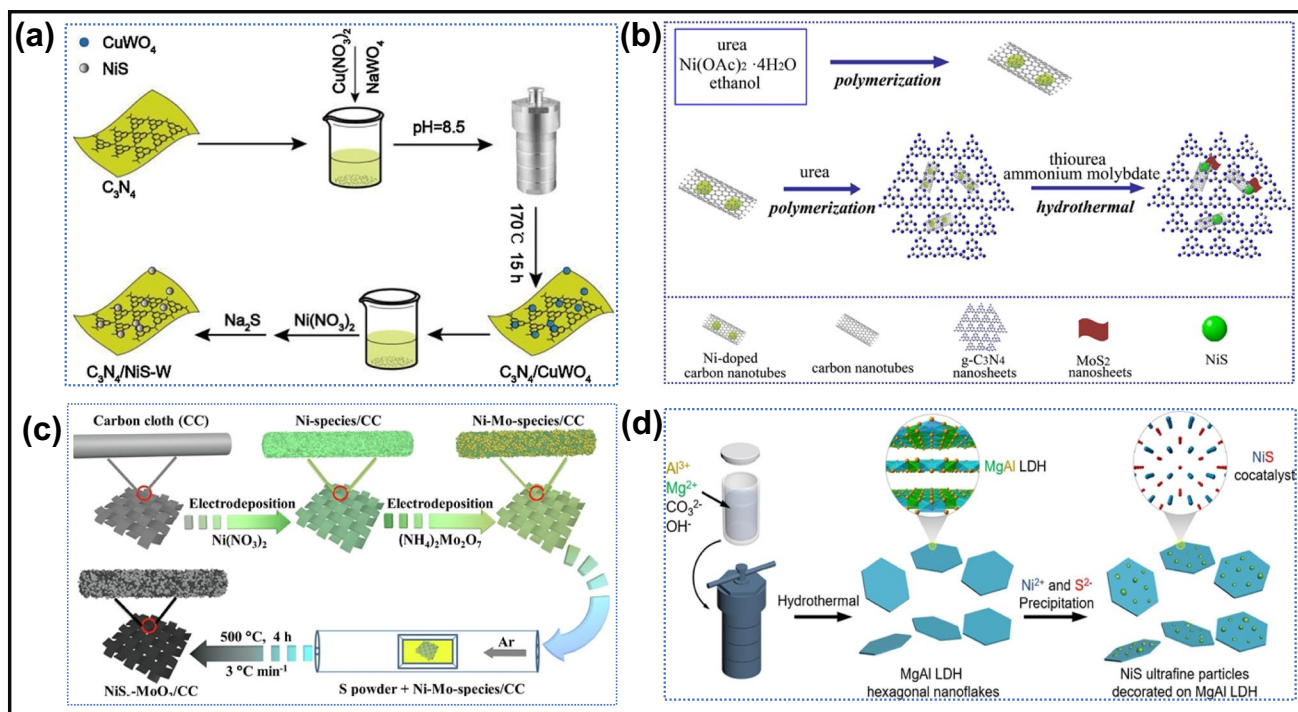
Fig. 4 Synthesis process of **a** g-C_3N_4/NiS-W. Reprinted with permission from (Xue et al. 2021) Copyright 2020 Elsevier. **b** NiS-MoS_2/CNTs/g-C_3N_4 hybrid. Reprinted with permission from ref. (Zhang et al. 2018b). Copyright 2018 Elsevier. **c** NiS_x-MoO_2/CC. Reprinted

with permission from ref. (Wang et al. 2020a). Copyright 2020 Elsevier. **d** MgAl-LDH/NiS heterostructures. Reprinted with permission from ref. (Chen et al. 2020a). Copyright 2019 Elsevier

also a low-cost and attractive material that when integrated with nickel sulfides that exhibited enhanced photocatalytic reactions. NiS-MoS_2/CNTs/g-C_3N_4 composite was synthesized by hydrothermal and polymerization treatment (Zhang et al. 2018b). Nickel (II) acetate tetra hydrate was used as the source of Ni^{2+} ions and NiS was generated by the reaction between nickel ions and thiourea. Firstly, Ni-CNTs/g-C_3N_4 was prepared via thermal polymerization and after that ammonium molybdate was used as the source of molybdenum followed by a hydrothermal treatment (Fig. 4b) to construct NiS_2-MoS_2/CNTs/g-C_3N_4. Layered double-metal hydroxides (LDHs) also act as good catalytic supports for NiS photocatalyst. NiS nanoparticles were decorated over pre-prepared 2D hexagonal nanoflakes by the precipitation method. Figure 4d shows the diagram illustrating the procedure for preparing MgAl-LDH/NiS heterostructure (Chen et al. 2020a). It is well known that the efficiency of a catalyst in any application is closely determined by the constitution as well as their morphological characteristics. The porous sponge-like structures provide a number of active sites, confinement effect, high surface area, and sufficient mass transfer and also prevent catalyst agglomeration (Peng et al. 2016; Li et al. 2019). A highly active carbon cloth decorated with NiS_x-MoO_2 nano-sponge was prepared and exhibited excellent electrocatalytic activity (Wang et al. 2020a). The

synthesis involved a two-step electro-deposition and was followed by vulcanization. NiS_x were grown directly on to the surface of MoO_2, and the coating process was eliminated in this synthesis route (Fig. 4c).

NiS_2-based photocatalysts

NiS_2 exist in two main phases, cubic and triclinic (Luo et al. 2017). Several heterostructure composites photocatalysts based on NiS_2 of various morphologies have been fabricated. A heterostructure of NiS_2 QDs with g-C_3N_4 using $NiCl_2$ and thiourea as Ni and S source respectively was fabricated. In the QDs-NiS_2/g-C_3N_4 heterojunction, NiS_2 was obtained with 200 plane having 0.20 interplanar spacing (Qin et al. 2020). In the other study, a hollow NiS_2 microspheres were synthesized by hydrothermal approach, and after annealing the prepared NiS_2 under mixed atmosphere (H_2 and Ar) conditions, mesoporous NiS was obtained by the reduction (Luo et al. 2017). The hollow microsphere structures of respective NiS and NiS_2 possessed large surface sites, which improved the photocatalytic activity properties (Fig. 5a–h). NiS_2 applicability as photocatalyst is limited due to its low charge transfer and high aggregation. To overcome these limitations, NiS_2 is employed with other semiconductors materials.
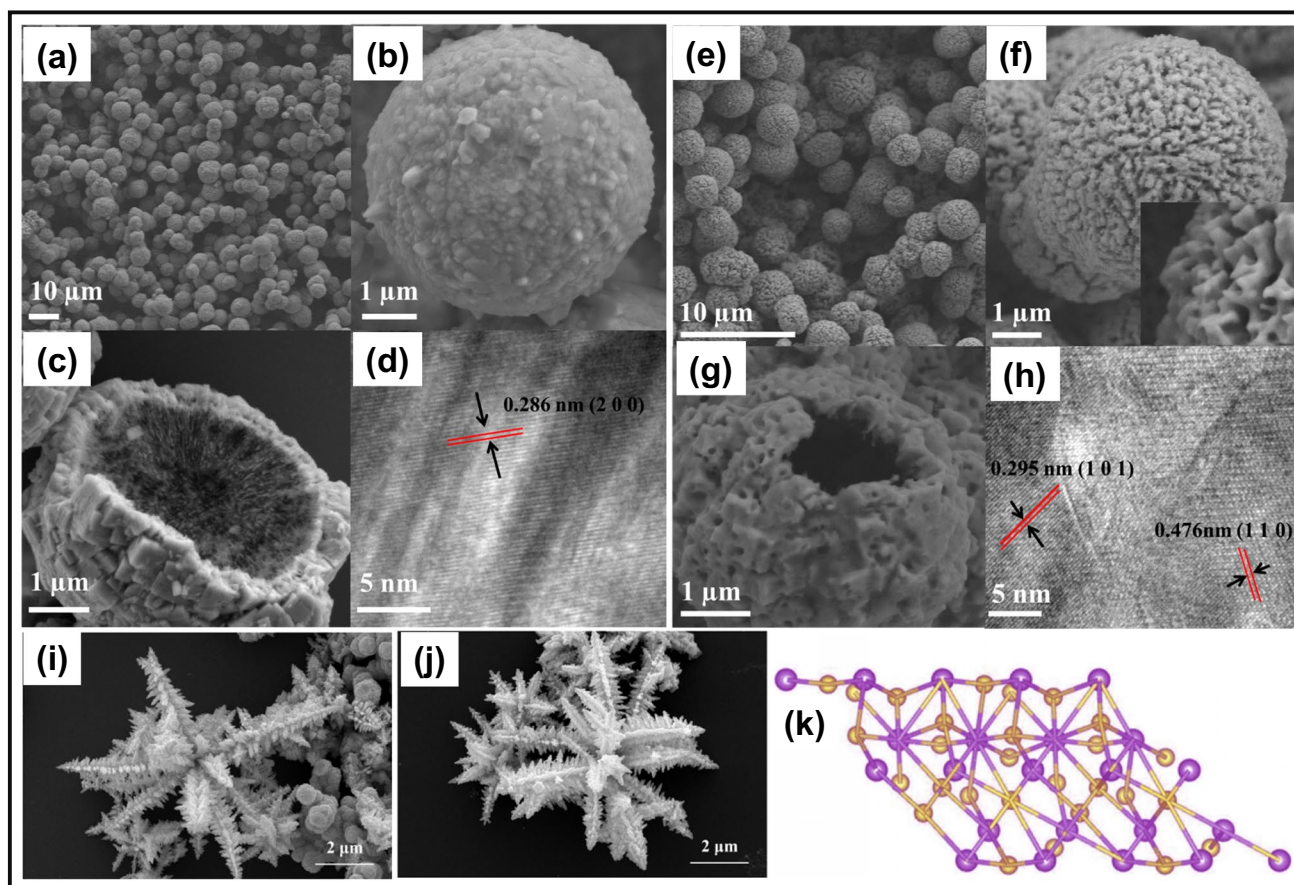
Fig. 5 Microspheres FESEM and TEM images of NiS₂ (**a–d**) and NiS (**e–i**). Reprinted with permission from ref. (Luo et al. 2017). Copyright 2016 American Chemical Society. **i–j** SEM images of pure CdS and NiS/CdS (Ni/Cd ratio of 0.4) nanoflowers. Reprinted with permission from ref. (Zhang et al. 2018a). Copyright 2019 Elsevier. **k** NiS₂ {111} crystal facets atomic structure from top and side view respectively (purple sphere represents Ni and orange sphere represents S atom). Reprinted with permission from ref. (Liang et al. 2020). Copyright 2019 Elsevier

Although metal-associated materials are originated with high activity, research view is towards metal-free materials to avoid secondary environmental issues. In this regard, carbon nitride found an advanced material which possesses not only good electrical properties but also remarkable photostability. Hybrid interface of g-C₃N₄ with NiS₂ improve the charge transfer, but the aggregation of the NiS₂ particles is achieved by the adoption of some suitable synthetic routes. A novel NiS₂/g-C₃N₄ is reported prepared by a simple hydrothermal method with the use of a low cost NiCl₂.6H₂O as Ni source and CS₂ as carbon source (Zhu et al. 2016). Engineering crystal facets is a hot research topic in photocatalysis. It has been observed from the reported works that synthesis of a particular facet is determined by the precursors used, solvent, and reaction parameters employed in the synthesis procedure (Zhang et al. 2022). For example, NiS₂ was prepared in two crystal facets, i.e., {111} and {100} where a hydrothermal treatment was given for 12 h at 150 °C to the reaction contents (Liang et al. 2020). When NiCl₂·6H₂O (96 mg) and Na₂S₂O₃·6H₂O (266 mg) along with 220 mg of polyvinylpyrrolidone (PVP) were used in deionized water, NiS₂ {111} was obtained, whereas NiS₂ {100} was observed on using Ni (NO₃)₂·6H₂O (1.4 g), CN₂H₄S (1.6 g), and 1.2 g PVP with 2 mg of NaOH. Figure 5k shows the atomic structure of NiS₂ {111} facet from both top and side views. In the other study, NiS/CdS heterostructures were prepared by adjusting the feed molar ratios of Ni/Cd from 0 to 1.2 and also varying the amounts of NaH₂PO₂·H₂O and lactic acid (Zhang et al. 2018a). NiS and CdS were obtained in β-rhombohedral and hexagonal phases respectively. The synthesized samples mainly composed of nanoflowers, and no appreciable change in the morphology was observed on changing Ni/Cd ratio as shown in Fig. 5i–j.

Applications of nickel sulfide-based photocatalysts

NiS and NiS₂-based photocatalysts for the degradation of organic compounds

NiS and NiS_2 nanostructures are the superior semiconductors and various photo-active materials took advantage of their semiconductor features in constructing composite catalysts and vouchsafed excellent photocatalytic activity towards organic compounds degradation (Zhu et al. 2016; Huerta-Flores et al. 2018; Ardebilchi Marand et al. 2020; Khan et al. 2021; Mohtar et al. 2021). Table 2 presents the survey scan summary on NiS and NiS_2-based photocatalytic degradation activities of different organic contaminants. The photocatalytic efficiency of nickel sulfide microstructures with different atomic ratios of Ni and S can be explained with the help of ANSYS simulation and field emission studies (Khan et al. 2021). It was observed that the sample having highest atomic ratio of Ni to S, i.e., 3:1, exhibited best performance in photodegradation (Khan et al. 2021). The probable reason may be associated with the morphologies of the samples. With increase in the atomic ratio of Ni, rod-like blocks increased and each rod behaves like an individual emitter. On the other side in S-rich samples, the single particles are not effective emitters; in fact, the whole tube behaves as the cold cathode, thus leading to higher emission properties. The obtained results are also supported by the ANSYS simulation and turn-on fields as shown in Fig. 6.

Several materials including organic and inorganic have been explored as supports for NiS and NiS_2-based photocatalysts with improved suppression rates of the recombination of e^-/h^+ pairs, thus resulting in higher photocatalytic efficiencies. Integrating NiS and NiS_2 with metal oxides is an effective approach towards designing active photocatalysts for the removal of organics (Saboo and Quadrelli 2019). Although nickel sulfide is of a high ability to harvest visible light due to their narrower band gaps, bare nickel sulfide suffers from the rapid recombining of charge carriers and photo-corrosion which affects its photocatalytic efficiency. Therefore, in this regard, nickel sulfides interfaced with other semiconductors behave like a co-catalyst, matching band edge positions lead to an efficient separation of e^-/h^+ pairs, thereby boosting the photocatalytic effect (Lee and Chang 2019). A remarkable adsorption and degradation of methyl orange was reported for heterostructure TiO_2/NiS_2 photocatalyst (Zhu et al. 2012). The higher surface area, porosity, and polarity match between the adsorbate and the adsorbent were found to be the major contributing factors. Similarly, in another report (Mahmood et al. 2019), incorporation of NiS_2 into TiO_2 increased the photodegradation efficiency from 17 to 80% for rhodamine B under visible light. Recently, a highly stable α-Fe_2O_3/NiS_2 composite achieved up to 93.7% degradation efficiency for humic acid which was higher than both the α-Fe_2O_3 and NiS_2 (Mohtar et al. 2021). The proposed degradation mechanism is depicted in Fig. 7a. Among the different proposed supports, magnetic materials like Fe_3O_4 are of prior importance because of large surface area and simple separation of the catalyst from the reaction system due to their paramagnetic behavior (Habibi-Yangjeh and Akhundi 2016). In the same direction, different conducting polymeric compounds are also regarded as promising materials due to their ease of preparation, high surface area and conductivity, and good environmental stability (Marimuthu et al. 2015). A polypyrrole@Fe_3O_4 core/shell as the support for NiS photocatalyst was fabricated and examined its photodegradation activity in cephalexin antibiotic removal under both direct sunlight and simulated UV irradiations (Torki and Faghihian 2017). The degradation efficiencies were determined to be 65 and 82% in sunlight and UV light respectively. The effect of irradiation time on cephalexin degradation by NiS and Fe_3O_4@PPY-NiS is shown in Fig. 7b.

Hybrid NiS/rGO composite formed by the adjacent interface of NiS and rGO stimulate the formation of charge carrier with higher life times and thus displayed the higher photocatalytic performance in degradation removal of methylene blue dye (Arumugam et al. 2020). A high photoactivity observed for the NiS/rGO was 87%, which was significantly higher than the NiS of 70% activity for the dye degradation. The electrochemical impedance spectroscopy (EIS) studies also confirmed the higher charge transfer efficiency for the NiS/rGO in comparison to NiS and reduced graphene oxide, respectively. In the NiS/rGO composite, rGO can act as electron acceptors which enhance the charge separation. Another work reported a highly active NiS/CNTs photocatalyst for methylene blue degradation within 50 min (Haider et al. 2021). The enhanced photoactivity of the hybrid photocatalyst than the individual NiS or CNTs was explained on the basis of generation of more reactive free radicals, surface defects, formed Ni–S–C bond, and availability of a greater number of active sites.

While dealing with NiS_2 photocatalyst, aggregation of the NPs is the main problem in the system. In this direction, g-C_3N_4, acts as a fascinating material owing to its s-triazine structure and visible light response (Zhu et al. 2016). This is due to the reason that heptazine rings of g-C_3N_4 serve as a good support for loading NiS_2 NPs and more importantly prevent the agglomeration of NiS_2 particles, thus improving the specific surface area and hence the photoactivity of the material. It is reported that the loading of NiS_2 over g-C_3N_4 is beneficial in improving the photoactivity especially because of the electron

Table 2 Photocatalytic removal of organic contaminants in the presence of nickel sulfide catalysts under different experimental conditions

Photocatalyst	Synthesis method	Morphology	Contaminant solution	Catalyst (mg)	Light source	Removal rate	Reference
NiS	Hydrothermal	Sponge-like	Methylene blue ($\sim 10^{-5}$ M) in 14 ml aqueous	5	Direct sunlight	99% (10 min)	(Molla et al. 2016)
NiS$_2$	Hydrothermal	Spherical	Indigo carmine (30 ppm) in 200 ml aqueous	200	450 W Xenon Lamp	51% (240 min)	(Huerta-Flores et al. 2018)
NiS	Sol–gel	Microtubes	Rhodamine B (10^{-5} M in 40 ml solution) Phenol (20 ppm, 40 ml solution)	30 22	40 W UV (Philips) tubes	96.72% (7 h) 88.84% (120 min)	(Khan et al. 2021)
NiS/SnS$_2$	Ball milling	Dispersed particles	Metronidazole (2 ppm, 10 ml solution)	25	60 W Tungsten lamp UV lamp	69.2% (240 min) 93.2% (240 min)	(Derikvandi and Nezamzadeh-Ejhieh 2017)
NiS-SiO$_2$	Ultrasound–microwave	Spherical particles	Methyl red	–	11 W UV lamp	85% (50 min)	(Hosseini et al. 2019)
Ni$_x$S$_y$/NiO	Solution combustion	Particles	Methylene blue (5 ppm, 100 ml)	35	Two 100-W Xenon lamps as visible light	52% (5 h)	(Ardebilchi Marand et al. 2020)
NiS/TiO$_2$	Sol–gel	Spherical particles	Sunset yellow (3×10^{-4} M, 50 ml)	200	Direct sunlight	98.90% (80 min)	(Rajamanickam et al. 2015)
NiS-TiO$_2$	Hydrothermal	Nanoflowers	Methyl orange (10 ppm, 30 ml)	30	500 W Xenon lamp	98% (20 min)	(Luo et al. 2020)
NiS/LaFeO$_3$	Hydrothermal	Nanoparticle-nanosheets	Methyl orange (20 ppm, 100 ml)	50	Direct sunlight	90% (120 min)	(Wang et al. 2020b)
MoS$_2$/NiS$_2$	Hydrothermal	Spherical shape-like sheets	Rhodamine B (20 ppm, 100 ml)	–	400 W Xenon lamp	90% (32 min)	(Harish et al. 2021)
AC-NiS/CoS	Chemical precipitation	Nanosheets	Methyl violet (10 ppm, 100 ml)	500	9 W LED lamps	98% (90 min)	(Artagan et al. 2021)
NiS/BiOBr	Hydrothermal	Nanoflakes	Rhodamine B (15 ppm, 200 ml)	20	450 W Xenon lamp	99% (50 min)	(Hu et al. 2020)
α-Fe$_2$O$_3$/NiS$_2$	Precipitation	Stacked plate-like	Humic acid (30 ppm, 100 ml)	10	300 W Xenon lamp	93.7% (100 min)	(Mohtar et al. 2021)
NiS$_2$/g-C$_3$N$_4$	Hydrothermal	Particles dispersed over sheets	Rhodamine B (10 ppm)	50	350 W xenon arc lamp	86% (210 min)	(Zhu et al. 2016)
NiS$_2$/RGO	Hydrothermal	Spherical particles dispersed over sheets	Cong red (10 g/L, 50 ml)	15	Direct sunlight	97.03% (40 min)	(Borthakur and Das 2018)
NiS/rGO	Hydrothermal and modified Hummer's method	Spherical particles over rGO layers	Amido Black dye (10 ppm, 100 ml)	100	500 W Tungsten halogen lamp	99% (120 min)	(Muninathan and Arumugam 2021)
NiS$_n$/FeOOH/BiVO$_4$	Hydrothermal	–	Phenol (0.43 mM, 100 ml)	100	400 W metal halogen lamp	53.4% (5 h)	(Huang et al. 2022)

Table 2 (continued)

Photocatalyst	Synthesis method	Morphology	Contaminant solution	Catalyst (mg)	Light source	Removal rate	Reference
NiS-PPY-Fe$_3$O$_4$	Polymerization and hydrothermal	Globular particles	Cephalexin (50 ppm)	–	UV Direct sunlight	82% (30 min) 65% (30 min)	(Torki and Faghihian 2017)
Co-doped/NiS/S-g-C$_3$N$_4$	Self-assembly method	Nanorods	Methylene blue	–	Visible light Xenon lamp	99% (32 min)	(Hakami 2022)
NiS/CNTs	Hydrothermal	Nanotubes dispersed over nanoparticles	Methylene blue (5 ppm, 50 ml)	5	200 W visible bulb	96% (50 min)	(Haider et al. 2021)
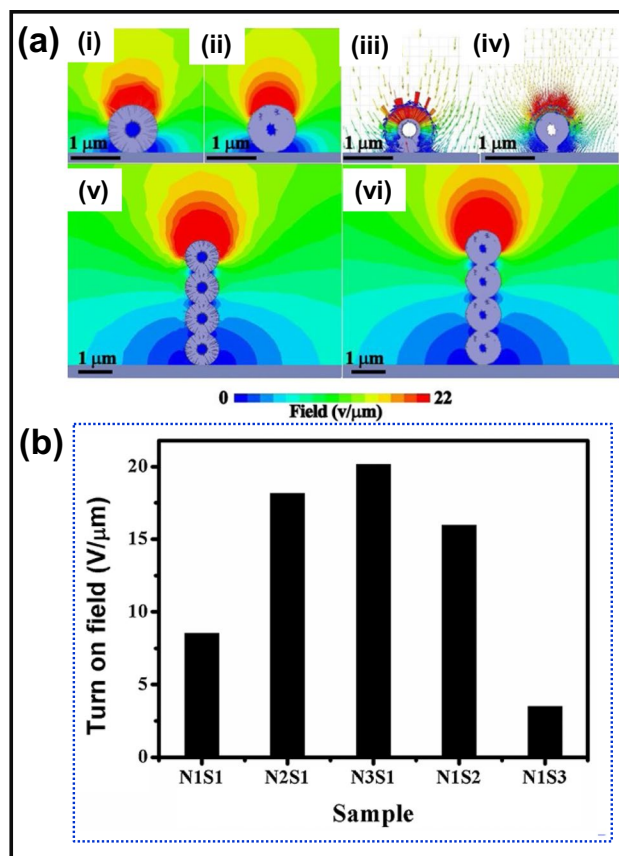
Fig. 6 a ANSYS simulations for output filed magnitude of nickel sulfide; individual rod-made sphere (i), particulate sphere (ii); field vectors for individual rod-made sphere (iii), particulate sphere (iv); and output filed magnitude for micro tube with rod-made sphere (v), particulate sphere (vi), and **b** turn-on fields for varying Ni to S atomic compositions (1 to 3). Reprinted with permission from ref. (Khan et al. 2021). Copyright 2021 Elsevier

transference from g-C$_3$N$_4$ to NiS$_2$ and decreasing the charge recombination rate (Zhu et al. 2016). NiS$_2$/g-C$_3$N$_4$ composite with improved absorption, less aggregation, and more charge transfer showed enhanced photocatalytic activity (Zhu et al. 2016). A 13.7 wt% NiS$_2$/g-C$_3$N$_4$ composite demonstrated the highest photocatalytic performance on rhodamine B underneath visible light illumination. Furthermore, doping g-C$_3$N$_4$ with non-metallic elements (O, B, S, P, and halogens) and then forming heterojunctions with metal doped-NiS is also an efficient way to improve the catalytic efficiency of NiS photocatalyst. A co-doped NiS/S-g-C$_3$N$_4$ heterojunction was synthesized and demonstrated an improved photocatalytic performance towards methylene blue degradation when compared to single photocatalysts (Hakami 2022). The results showed that the interface contact between Co-NiS nanorods and S-g-C$_3$N$_4$ nanosheets increased the formation and separation effectiveness of the photoexcited charge carriers, thus preventing their recombination.
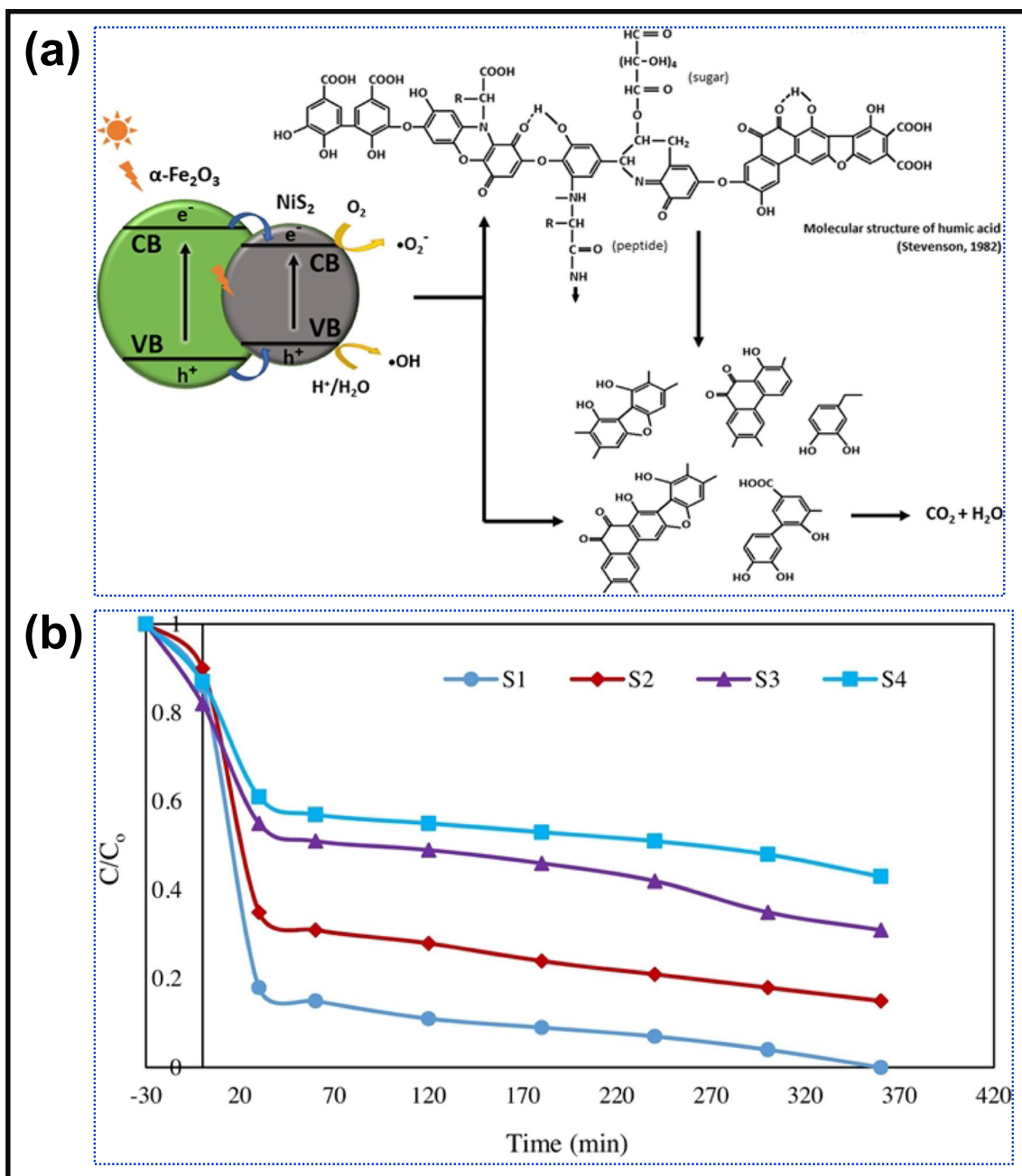
Fig. 7 a Photocatalytic mechanism of humic acid degradation by α-Fe$_2$O$_3$/NiS$_2$ photocatalyst. Reprinted with permission from ref. (Mohtar et al. 2021) Copyright 2021 Elsevier. **b** Cephalexin degrada-tion by NiS and Fe$_3$O$_4$@PPY-NiS; S4 and S2 (sunlight) and S3 and S1 (UV) irradiations respectively. Reprinted with permission from ref. (Torki and Faghihian 2017). Copyright 2017 Elsevier

Amorphous polysulfide, NiS$_x$, also acts as a good co-catalyst. Both Ni (OH)$_2$ and NiS$_x$ have been reported as highly active co-catalyst with bismuth vanadate (BiVO$_4$) in the photodegradation of phenol due to effective elec-tron transfer (Huang et al. 2022). As already described, phase and size of the synthesized nanoparticles (NPs) can be regulated by varying the initial ration of the concentra-tions of the used sources. Single-phase nickel sulfide NPs

including NiS, Ni$_3$S$_4$, NiS$_2$, and Ni$_7$S$_6$ were obtained utiliz-ing a temperature-controlled precursor injection procedure (Karthikeyan et al. 2015). The synthesized NiS-phase NPs exhibited metallic characteristics and highest reduction effi-ciency towards 4-nitrophenol when compared with the other nickel sulfide phases. A complete reduction of 4-nitrophe-nol into 4-aminophenol was achieved in 300 s (Karthikeyan et al. 2015). On the other hand, the removal efficiencies of

other sulfur-rich phases were found lesser than that of the NiS phase being in 400 and 500 s for (NiS_2, Ni_3S_4) and Ni_7S_6 respectively. In recent times, crystal facet-dependent materials are receiving tremendous attention in the field of photocatalysis. It is found that a particular faceted nanocrystals exhibit greater photoactivity than the other facets of the same material. Liang et al. found NiS_2 {111} nanocrystals exhibiting better photocatalytic activity in degrading of methyl orange and methylene blue organic dyes than {100} faceted nanocrystals (Liang et al. 2020). Moreover, integrating NiS_2 {111} with (rGO) further enhanced the photocatalytic efficiency where complete removal was achieved in 150 and 180 min respectively.

Conclusion and future perspectives

This review presents the recent progress and developments in nickel sulfide (NiS and NiS_2)-based photocatalysts, focusing on the applications in environmental degradation of model organic wastewater pollutants by photocatalytic process. Undoubtedly, both NiS and NiS_2 can be considered as superior active visible-light semiconductors, due to their narrow indirect bandgap, which have demonstrated promising inherent photocatalytic properties.

NiS and NiS_2 both possesses the characteristics to be an efficient photocatalyst with a limitation of fast recombination rates of photogenerated charge carriers which need to be improved for a better performance. Hence, much effort has been directed to towards co-catalyst in constructing heterostructures interfaces with enhanced photocatalytic properties. The analyzed properties of NiS and NiS_2 can be extended to make the perception of inherent effects of heterostructure composite photocatalysts easy, paving the course of designing photocatalysts with improved photocatalytic activity and higher performance in the degradation of various organic wastewater pollutants. NiS and NiS_2 hybridized with metal oxides, metals, and carbon-based materials and further leads multicomponent from binary to ternary heterostructures which causes band edge alignments and improved heterostructures and surface characteristics with enhanced photocatalytic properties. The overall survey scan of the literature highlighted significant improvements on hetero-interfaced photocatalysts based on NiS and NiS_2 that are comparable to expensive noble-metal photocatalysts and degradation activity of organics. This compiled literature advancements in NiS and NiS_2 photocatalysts for the environment will provide a comprehensive insight for developing new approach of designing superior visible-light photoactive catalysts based on cost-efficient nickel metal cocatalysts.

Although current studies have reported significant improvements in the catalytic efficiency of the heterostructures in water treatment, the active components of the catalyst will inevitably be lost or poisoned after multiple cycles. Therefore, there is need to improve the stability and reusability of the catalysts. In the future, more optimized synthetic methods should be developed for the stable heterostructured materials.

There are fewer studies on the eco-toxicity of nickel sulfide-based materials. Analysis of eco-toxicity is favorable for establishing more environmentally friendly catalytic systems.

DFT computations can provide in-depth view of the transformation of target pollutants and help us to accurately elucidate the active catalytic centers.

Overall, the study on nickel sulfide-based heterostructures is still at an early stage; it is far from the large-scale practical application. Studies on stability for long-term performance, incorporation on structural modelling of pure structures of NiS and NiS_2, and their heterostructures are encouraged for further advancements in comprehending these photocatalytic materials for potential industrial implementations.

Declarations

Ethical approval Not applicable. The research did not involve human participants or animals.

Consent for publication We have reviewed the final version of the manuscript and approved it for publication.

Competing interests The authors declare no competing interests.

References

Adhikari R, Gyawali G, Sekino T, Wohn Lee S (2013) Microwave assisted hydrothermal synthesis of Ag/AgCl/WO3 photocatalyst and its photocatalytic activity under simulated solar light. J Solid State Chem 197:560–565. https://doi.org/10.1016/j.jssc.2012.08.012

Akshatha S, Sreenivasa S, Kumar KY et al (2020) Rutile, mesoporous ruthenium oxide decorated graphene oxide as an efficient visible light driven photocatalyst for hydrogen evolution reaction and organic pollutant degradation. Mater Sci Semicond Process 116:105156. https://doi.org/10.1016/j.mssp.2020.105156

Alrobei H, Prashanth MK, Manjunatha CR et al (2021) Adsorption of anionic dye on eco-friendly synthesised reduced graphene oxide anchored with lanthanum aluminate: isotherms, kinetics

and statistical error analysis. Ceram Int 47:10322–10331. https://doi.org/10.1016/j.ceramint.2020.07.251

Anwer H, Mahmood A, Lee J et al (2019) Photocatalysts for degradation of dyes in industrial effluents: opportunities and challenges. Nano Res 12:955–972. https://doi.org/10.1007/s12274-019-2287-0

Ardebilchi Marand N, Masoudpanah SM, Bafghi MSh, Alamolhoda S (2020) Photocatalytic activity of nickel sulfide composite powders synthesized by solution combustion method. J Electron Mater 49:1266–1272. https://doi.org/10.1007/s11664-019-07744-z

Artagan Ö, Vaizoğullar Aİ, Uğurlu M (2021) Activated carbon-supported NiS/CoS photocatalyst for degradation of methyl violet (MV) and selective disinfection process for different bacteria under visible light irradiation. J Taibah Univ Sci 15:154–169. https://doi.org/10.1080/16583655.2021.1930718

Arumugam P, Sengodan P, Duraisamy N et al (2020) An effective strategy to enhance the photocatalytic performance by forming NiS/rGO heterojunction nanocomposites. Ionics 26:4201–4212. https://doi.org/10.1007/s11581-020-03564-y

Balayeva OO, Azizov AA, Muradov MB et al (2017) Effect of thermal annealing on the properties of nickel sulfide nanostructures: structural phase transition. Mater Sci Semicond Process 64:130–136. https://doi.org/10.1016/j.mssp.2017.03.021

Borthakur P, Das MR (2018) Hydrothermal assisted decoration of NiS2 and CoS nanoparticles on the reduced graphene oxide nanosheets for sunlight driven photocatalytic degradation of azo dye: effect of background electrolyte and surface charge. J Colloid Interface Sci 516:342–354. https://doi.org/10.1016/j.jcis.2018.01.050

Chandra Patel P, Kumar Mishra P, Kandpal HC (2021) Low temperature magnetic study of α-NiS nanoparticles synthesized via hydrothermal technique. Mater Today: Proceedings 47:1550–1556. https://doi.org/10.1016/j.matpr.2021.03.499

Chen J, Wang C, Zhang Y et al (2020) Engineering ultrafine NiS cocatalysts as active sites to boost photocatalytic hydrogen production of MgAl layered double hydroxide. Appl Surf Sci 506:144999. https://doi.org/10.1016/j.apsusc.2019.144999

Chen Y, Jiang H, Li L et al (2020b) Hierarchical NiS decorated CuO@ZnFe2O4 nanoarrays as advanced photocathodes for hydrogen evolution reaction. Int J Hydrogen Energy 45:6174–6183. https://doi.org/10.1016/j.ijhydene.2019.12.170

Derikvandi H, Nezamzadeh-Ejhieh A (2017) Designing of experiments for evaluating the interactions of influencing factors on the photocatalytic activity of NiS and SnS2: focus on coupling, supporting and nanoparticles. J Colloid Interface Sci 490:628–641. https://doi.org/10.1016/j.jcis.2016.11.102

Dhiman P, Rana G, Kumar A et al (2022) ZnO-based heterostructures as photocatalysts for hydrogen generation and depollution: a review. Environ Chem Lett 20:1047–1081. https://doi.org/10.1007/s10311-021-01361-1

Ding L, Li D, Shen H et al (2021) 2D β-NiS as electron harvester anchors on 2D ZnIn2S4 for boosting photocatalytic hydrogen production. J Alloys Compd 853:157328. https://doi.org/10.1016/j.jallcom.2020.157328

Dong W, An L, Wang X et al (2011) Controlled synthesis and morphology evolution of nickel sulfide micro/nanostructure. J Alloy Compd 509:2170–2175. https://doi.org/10.1016/j.jallcom.2010.10.178

Emadi H, Salavati-Niasari M, Sobhani A (2017) Synthesis of some transition metal (M: 25Mn, 27Co, 28Ni, 29Cu, 30Zn, 47Ag, 48Cd) sulfide nanostructures by hydrothermal method. Adv Coll Interface Sci 246:52–74. https://doi.org/10.1016/j.cis.2017.06.007

Gan X, Lei D, Ye R et al (2021) Transition metal dichalcogenide-based mixed-dimensional heterostructures for visible-light-driven photocatalysis: dimensionality and interface engineering. Nano Res 14:2003–2022. https://doi.org/10.1007/s12274-020-2955-x

Ghezelbash A, Sigman MB, Korgel BA (2004) Solventless synthesis of nickel sulfide nanorods and triangular nanoprisms. Nano Lett 4:537–542. https://doi.org/10.1021/nl035067+

Gou J, Xie S, Yang Z et al (2017) A high-performance supercapacitor electrode material based on NiS/Ni 3 S 4 composite. Electrochim Acta 229:299–305. https://doi.org/10.1016/j.electacta.2017.01.111

Habibi-Yangjeh A, Akhundi A (2016) Novel ternary g -C 3 N 4 /Fe 3 O 4 /Ag 2 CrO 4 nanocomposites: magnetically separable and visible-light-driven photocatalysts for degradation of water pollutants. J Mol Catal A: Chem 415:122–130. https://doi.org/10.1016/j.molcata.2016.01.032

Haider S, Shar SS, Shakir I, Agboola PO (2021) Design of NiS/CNTs nanocomposites for visible light driven catalysis and antibacterial activity studies. Ceram Int 47:34269–34277. https://doi.org/10.1016/j.ceramint.2021.08.337

Hakami O (2022) Construction of Co-doped NiS/S-g-C3N4 heterojunction for boosting degradation of dye and inactivation of pathogens in visible light. J Photochem Photobiol A Chem 425:113704. https://doi.org/10.1016/j.jphotochem.2021.113704

Han Y, Zhang Q, Liang Z et al (2020) Mn0.3Cd0.7S nanorods modified with NiS clusters as photocatalysts for the H2 evolution reaction. J Mater Sci 55:5390–5401. https://doi.org/10.1007/s10853-020-04405-z

Han Y, Chen Y, Fan R et al (2021) Promotion effect of metal phosphides towards electrocatalytic and photocatalytic water splitting. Eco Mat 3:e12097. https://doi.org/10.1002/eom2.12097

Harish S, Bharathi P, Prasad P et al (2021) Interface enriched highly interlaced layered MoS 2 /NiS 2 nanocomposites for the photocatalytic degradation of rhodamine B dye. RSC Adv 11:19283–19293. https://doi.org/10.1039/D1RA01094D

Hosseini M, Fazelian N, Fakhri A et al (2019) Preparation, and structural of new NiS-SiO2 and Cr2S3-TiO2 nano-catalyst: photocatalytic and antimicrobial studies. J Photochem Photobiol, B 194:128–134. https://doi.org/10.1016/j.jphotobiol.2019.03.016

Hu M, Yan A, Cui Q et al (2020) NiS/BiOBr hybrids with retarded carrier recombination and enhanced visible-light-driven photocatalytic activity. J Mater Sci 55:4265–4278. https://doi.org/10.1007/s10853-019-04288-9

Hu Q, Zhang S, Li W et al (2022) Regulating the structure and morphology of nickel sulfides for electrochemical energy storage: the role of solvent pH. Chem Eng J 441:136130. https://doi.org/10.1016/j.cej.2022.136130

Hu Q, Zhang S, Zou X et al (2022b) Coordination agent-dominated phase control of nickel sulfide for high-performance hybrid supercapacitor. J Colloid Interface Sci 607:45–52. https://doi.org/10.1016/j.jcis.2021.08.185

Huang Z-Y, Li X-X, Liu Z-J et al (2015) Morphology effect on the kinetic parameters and surface thermodynamic properties of Ag 3 PO 4 micro-/nanocrystals. J Nanomater 2015:1–9. https://doi.org/10.1155/2015/743121

Huang X, Chen M, Wang Y et al (2022) Amorphous NiSn and FeOOH as bifunctional co-catalysts for oxygen reduction and phenol (water) oxidation over BiVO4 under visible light. J Hazard Mater 421:126650. https://doi.org/10.1016/j.jhazmat.2021.126650

Huerta-Flores AM, Torres-Martínez LM, Moctezuma E et al (2018) Green synthesis of earth-abundant metal sulfides (FeS2, CuS, and NiS2) and their use as visible-light active photocatalysts for H2 generation and dye removal. J Mater Sci: Mater Electron 29:11613–11626. https://doi.org/10.1007/s10854-018-9259-x

Idris NH, Rahman MM, Chou S-L et al (2011) Rapid synthesis of binary α-NiS–β-NiS by microwave autoclave for rechargeable lithium batteries. Electrochim Acta 58:456–462. https://doi.org/10.1016/j.electacta.2011.09.066

Izzudin NM, Jalil AA, Aziz FFA et al (2021) Simultaneous remediation of hexavalent chromium and organic pollutants in wastewater using period 4 transition metal oxide-based photocatalysts: a review. Environ Chem Lett 19:4489–4517. https://doi.org/10.1007/s10311-021-01272-1

Jiang L, Wang K, Wu X et al (2019) Amorphous bimetallic cobalt nickel sulfide cocatalysts for significantly boosting photocatalytic hydrogen evolution performance of graphitic carbon nitride: efficient interfacial charge transfer. ACS Appl Mater Interfaces 11:26898–26908. https://doi.org/10.1021/acsami.9b07311

Karthikeyan R, Thangaraju D, Prakash N, Hayakawa Y (2015) Single-step synthesis and catalytic activity of structure-controlled nickel sulfide nanoparticles. CrystEngComm 17:5431–5439. https://doi.org/10.1039/C5CE00742A

Khan S, Choi H, Kim D et al (2020) Self-assembled heterojunction of metal sulfides for improved photocatalysis. Chem Eng J 395:125092. https://doi.org/10.1016/j.cej.2020.125092

Khan R, Das NS, Das B et al (2021) Hierarchical nickel sulphide microstructures for controlled water disinfection and cold cathode emission. J Photochem Photobiol A Chem 412:113212. https://doi.org/10.1016/j.jphotochem.2021.113212

Kumar A, Thakur PR, Sharma G et al (2019a) Carbon nitride, metal nitrides, phosphides, chalcogenides, perovskites and carbides nanophotocatalysts for environmental applications. Environ Chem Lett 17:655–682. https://doi.org/10.1007/s10311-018-0814-8

Kumar M, RaoT S, Isloor AM et al (2019b) Use of cellulose acetate/polyphenylsulfone derivatives to fabricate ultrafiltration hollow fiber membranes for the removal of arsenic from drinking water. Int J Biol Macromol 129:715–727. https://doi.org/10.1016/j.ijbiomac.2019.02.017

Kumari V, Sharma S, Sharma A et al (2021) Hydrothermal synthesis conditions effect on hierarchical ZnO/CuO hybrid materials and their photocatalytic activity. J Mater Sci: Mater Electron. https://doi.org/10.1007/s10854-021-05622-1

Kummu M, Guillaume JHA, de Moel H et al (2016) The world's road to water scarcity: shortage and stress in the 20th century and pathways towards sustainability. Sci Rep 6:38495. https://doi.org/10.1038/srep38495

Lee SL, Chang C-J (2019) Recent progress on metal sulfide composite nanomaterials for photocatalytic hydrogen production. Catalysts 9:457. https://doi.org/10.3390/catal9050457

Li D, Li X, Hou X et al (2014) Building a Ni_3S_2 nanotube array and investigating its application as an electrode for lithium ion batteries. Chem Commun 50:9361–9364. https://doi.org/10.1039/C4CC01311E

Li Z, Meng X, Zhang Z (2018) Recent development on MoS2-based photocatalysis: a review. J Photochem Photobiol, C 35:39–55. https://doi.org/10.1016/j.jphotochemrev.2017.12.002

Li Y, Yu H, Wang Z et al (2019) Boron-doped silver nanosponges with enhanced performance towards electrocatalytic nitrogen reduction to ammonia. Chem Commun 55:14745–14748. https://doi.org/10.1039/C9CC07232B

Li N, Ai L, Jiang J, Liu S (2020) Spinel-type oxygen-incorporated Ni3+ self-doped Ni3S4 ultrathin nanosheets for highly efficient and stable oxygen evolution electrocatalysis. J Colloid Interface Sci 564:418–427. https://doi.org/10.1016/j.jcis.2019.12.036

Liang Y, Yang Y, Xu K et al (2020) Crystal facets engineering and rGO hybridizing for synergistic enhancement of photocatalytic activity of nickel disulfide. J Hazard Mater 384:121402. https://doi.org/10.1016/j.jhazmat.2019.121402

Lichtfouse E, Morin-Crini N, Bradu C et al (2021) Technologies to remove selenium from water and wastewater. In: Morin-Crini N, Lichtfouse E, Crini G (eds) Emerging Contaminants, vol 2. Springer International Publishing, Cham, pp 207–304

Lim WP, Wong CT, Ang SL et al (2006) Phase-selective synthesis of copper sulfide nanocrystals. Chem Mater 18:6170–6177. https://doi.org/10.1021/cm061686i

Liu X, Li J (2021) A method for effectively regulating the green emissions of ZnO through NiS@NiO/rGO. Appl Surf Sci 556:149805. https://doi.org/10.1016/j.apsusc.2021.149805

Liu Z, Zhou M (2020) Co-modification with cost-effective nickel oxides and nickel sulfides on $CuInS_2$ nanosheets photocathode for enhanced photoelectrochemical performance. ACS Sustain Chem Eng 8:512–519. https://doi.org/10.1021/acssuschemeng.9b05936

Liu X, Bie C, He B et al (2021) 0D/2D NiS/CdS nanocomposite heterojunction photocatalyst with enhanced photocatalytic H2 evolution activity. Appl Surf Sci 554:149622. https://doi.org/10.1016/j.apsusc.2021.149622

Lopes JL, Martins MJ, Nogueira HIS et al (2021) Carbon-based heterogeneous photocatalysts for water cleaning technologies: a review. Environ Chem Lett 19:643–668. https://doi.org/10.1007/s10311-020-01092-9

Luo P, Zhang H, Liu L et al (2017) Targeted synthesis of unique nickel sulfide (NiS, NiS_2) microarchitectures and the applications for the enhanced water splitting system. ACS Appl Mater Interfaces 9:2500–2508. https://doi.org/10.1021/acsami.6b13984

Luo Y-N, Li Y, Qian L et al (2020) Excellent photocatalytic performance from NiS decorated TiO2 nanoflowers with exposed 001 facets. Mater Res Bull 130:110945. https://doi.org/10.1016/j.materresbull.2020.110945

Luo Q, Lu C, Liu L, Zhu M (2023) A review on the synthesis of transition metal nitride nanostructures and their energy related applications. Green Energy Environ 8:406–437. https://doi.org/10.1016/j.gee.2022.07.002

Mabuea BP, Swart HC, Erasmus E (2022) Photocatalytic decomposition of an azo dye using transition-metal-doped tungsten and molybdenum carbides. ACS Omega 7:23401–23411. https://doi.org/10.1021/acsomega.2c01727

Mahmood PH, Amiri O, Ahmed SS, Hama JR (2019) Simple microwave synthesis of TiO2/NiS2 nanocomposite and TiO2/NiS2/Cu nanocomposite as an efficient visible driven photocatalyst. Ceram Int 45:14167–14172. https://doi.org/10.1016/j.ceramint.2019.04.118

Manjunatha C, Srinivasa N, Chaitra SK et al (2020) Controlled synthesis of nickel sulfide polymorphs: studies on the effect of morphology and crystal structure on OER performance. Mater Today Energy 16:100414. https://doi.org/10.1016/j.mtener.2020.100414

Marimuthu T, Mohamad S, Alias Y (2015) Needle-like polypyrrole–NiO composite for non-enzymatic detection of glucose. Synth Met 207:35–41. https://doi.org/10.1016/j.synthmet.2015.06.007

Meng S, Zhang J, Chen S et al (2019) Perspective on construction of heterojunction photocatalysts and the complete utilization of photogenerated charge carriers. Appl Surf Sci 476:982–992. https://doi.org/10.1016/j.apsusc.2019.01.246

Mishra M, Chun D-M (2015) α-Fe2O3 as a photocatalytic material: a review. Appl Catal A 498:126–141. https://doi.org/10.1016/j.apcata.2015.03.023

Mittal A, Sharma S, Kumari V et al (2019) Highly efficient, visible active TiO2/CdS/ZnS photocatalyst, study of activity in an ultra low energy consumption LED based photo reactor. J Mater Sci: Mater Electron 30:17933–17946. https://doi.org/10.1007/s10854-019-02147-6

Mohtar SS, Aziz F, Nor ARM et al (2021) Photocatalytic degradation of humic acid using a novel visible-light active α-Fe2O3/NiS2 composite photocatalyst. J Environ Chem Eng 9:105682. https://doi.org/10.1016/j.jece.2021.105682

Molla A, Sahu M, Hussain S (2016) Synthesis of tunable band gap semiconductor nickel sulphide nanoparticles: rapid and round

the clock degradation of organic dyes. Sci Rep 6:26034. https://doi.org/10.1038/srep26034

Muninathan S, Arumugam S (2021) Enhanced photocatalytic activities of NiS decorated reduced graphene oxide for hydrogen production and toxic dye degradation under visible light irradiation. Int J Hydrogen Energy 46:6532–6546. https://doi.org/10.1016/j.ijhydene.2020.11.178

Muniyappa M, Kalegowda SN, Shetty M et al (2022) Cocatalyst free nickel sulphide nanostructure for enhanced photocatalytic hydrogen evolution. Int J Hydrogen Energy 47:5307–5318. https://doi.org/10.1016/j.ijhydene.2021.11.171

Nawaz A, Atif M, Khan A et al (2023) Solar light driven degradation of textile dye contaminants for wastewater treatment – studies of novel polycationic selenide photocatalyst and process optimization by response surface methodology desirability factor. Chemosphere 328:138476. https://doi.org/10.1016/j.chemosphere.2023.138476

Okpara EC, Olatunde OC, Wojuola OB, Onwudiwe DC (2023) Applications of transition metal oxides and chalcogenides and their composites in water treatment: a review. Environ Adv 11:100341. https://doi.org/10.1016/j.envadv.2023.100341

Ong W-J, Tan L-L, Ng YH et al (2016) Graphitic carbon nitride (g-C$_3$N$_4$)-based photocatalysts for artificial photosynthesis and environmental remediation: are we a step closer to achieving sustainability? Chem Rev 116:7159–7329. https://doi.org/10.1021/acs.chemrev.6b00075

Passi M, Pal B (2021) A review on CaTiO3 photocatalyst: activity enhancement methods and photocatalytic applications. Powder Technol 388:274–304. https://doi.org/10.1016/j.powtec.2021.04.056

Peng X, Chen D, Yang X et al (2016) Microwave-assisted synthesis of highly dispersed PtCu nanoparticles on three-dimensional nitrogen-doped graphene networks with remarkably enhanced methanol electrooxidation. ACS Appl Mater Interfaces 8:33673–33680. https://doi.org/10.1021/acsami.6b11800

Peters AW, Li Z, Farha OK, Hupp JT (2016) Toward inexpensive photocatalytic hydrogen evolution: a nickel sulfide catalyst supported on a high-stability metal–organic framework. ACS Appl Mater Interfaces 8:20675–20681. https://doi.org/10.1021/acsami.6b04729

Qian L-L, Li Y, Li J, Wang C-W (2018) Enhanced photocatalytic performance from NiS/TiO2 p-n heterojunction nanosheet arrays. Superlattices Microstruct 117:317–329. https://doi.org/10.1016/j.spmi.2018.03.060

Qin H, Guo R-T, Liu X-Y et al (2020) 0D NiS2 quantum dots modified 2D g-C3N4 for efficient photocatalytic CO2 reduction. Colloids Surf A Physicochem Eng Asp 600:124912. https://doi.org/10.1016/j.colsurfa.2020.124912

Rajamanickam D, Dhatshanamurthi P, Shanthi M (2015) Enhanced photocatalytic efficiency of NiS/TiO2 composite catalysts using sunset yellow, an azo dye under day light illumination. Mater Res Bull 61:439–447. https://doi.org/10.1016/j.materresbull.2014.09.095

Rao CNR, Pisharody KPR (1976) Transition metal sulfides. Prog Solid State Chem 10:207–270. https://doi.org/10.1016/0079-6786(76)90009-1

Rashid M, Mowla D, Esmaeilzadeh F et al (2021) Boosted Cr(VI) clean up over magnetically recoverable NiS/γ-Fe2O3/C type-II heterostructure derived from bimetal (Fe/Ni)-organic framework under visible light. J Clean Prod 317:128471. https://doi.org/10.1016/j.jclepro.2021.128471

Rhodes JM, Jones CA, Thal LB, Macdonald JE (2017) Phase-controlled colloidal syntheses of iron sulfide nanocrystals via sulfur precursor reactivity and direct pyrite precipitation. Chem Mater 29:8521–8530. https://doi.org/10.1021/acs.chemmater.7b03550

Roffey A, Hollingsworth N, Islam H-U et al (2016) Phase control during the synthesis of nickel sulfide nanoparticles from dithiocarbamate precursors. Nanoscale 8:11067–11075. https://doi.org/10.1039/C6NR00053C

Saboo T, Quadrelli EA (2019) Photoproduction of ammonia. Stud Surf Sci Catal 178:47–63. https://doi.org/10.1016/B978-0-444-64127-4.00003-3

Sharma S, Kumar N, Mari B et al (2021a) Solution combustion synthesized TiO2/Bi2O3/CuO nano-composites and their photocatalytic activity using visible LEDs assisted photoreactor. Inorg Chem Commun 125:108418. https://doi.org/10.1016/j.inoche.2020.108418

Sharma S, Mittal A, Singh Chauhan N et al (2021b) Developments in visible-light active TiO2/SnX (X = S and Se) and their environmental photocatalytic applications – a mini-review. Inorg Chem Commun 133:108874. https://doi.org/10.1016/j.inoche.2021.108874

Sharma S, Kumar N, Makgwane PR et al (2022) TiO2/SnO2 nano-composite: new insights in synthetic, structural, optical and photocatalytic aspects. Inorg Chim Acta 529:120640. https://doi.org/10.1016/j.ica.2021.120640

Shi X, Ling X, Li L et al (2019) Nanosheets assembled into nickel sulfide nanospheres with enriched Ni^{3+} active sites for efficient water-splitting and zinc–air batteries. J Mater Chem A 7:23787–23793. https://doi.org/10.1039/C9TA03819A

Shombe GB, Khan MD, Zequine C et al (2020) Direct solvent free synthesis of bare α-NiS, β-NiS and α-β-NiS composite as excellent electrocatalysts: effect of self-capping on supercapacitance and overall water splitting activity. Sci Rep 10:3260. https://doi.org/10.1038/s41598-020-59714-9

Shriber P, Tkachev M, Atkins A et al (2022) Synthesis of nickel sulfide dendrites from nickel foil using thermal annealing. Materialia 21:101316. https://doi.org/10.1016/j.mtla.2022.101316

Soltani N, Saion E, Hussein MZ et al (2012) Visible light-induced degradation of methylene blue in the presence of photocatalytic ZnS and CdS nanoparticles. IJMS 13:12242–12258. https://doi.org/10.3390/ijms131012242

Su T, Xiao L, Gao Y et al (2019) Multifunctional MoS$_2$ ultrathin nano-flakes loaded by Cd$_{0.5}$Zn$_{0.5}$S QDs for enhanced photocatalytic H$_2$ production. Int J Energy Res 43:5678–5686. https://doi.org/10.1002/er.4596

Sun X (2003) Microstructure studies on hexagonal layered Ni-S nanocrystals. Appl Surf Sci 217:23–27. https://doi.org/10.1016/S0169-4332(03)00566-X

Tang C, Pu Z, Liu Q et al (2015) Ni3S2 nanosheets array supported on Ni foam: a novel efficient three-dimensional hydrogen-evolving electrocatalyst in both neutral and basic solutions. Int J Hydrogen Energy 40:4727–4732. https://doi.org/10.1016/j.ijhydene.2015.02.038

Torki F, Faghihian H (2017) Sunlight-assisted decomposition of cephalexin by novel synthesized NiS-PPY-Fe$_3$O$_4$ nanophotocatalyst. J Photochem Photobiol, A 338:49–59. https://doi.org/10.1016/j.jphotochem.2017.02.003

Wang J, Chew SY, Wexler D et al (2007) Nanostructured nickel sulfide synthesized via a polyol route as a cathode material for the rechargeable lithium battery. Electrochem Commun 9:1877–1880. https://doi.org/10.1016/j.elecom.2007.04.020

Wang Q, Yun G, Bai Y et al (2014) CuS, NiS as co-catalyst for enhanced photocatalytic hydrogen evolution over TiO2. Int J Hydrogen Energy 39:13421–13428. https://doi.org/10.1016/j.ijhydene.2014.04.020

Wang B, Pan J, Jiang Z et al (2018) The bimetallic iron−nickel sulfide modified g-C3N4 nano-heterojunction and its photocatalytic hydrogen production enhancement. J Alloy Compd 766:421–428. https://doi.org/10.1016/j.jallcom.2018.06.377

Wang X, Xie Y, Jiao Y et al (2019) Carbon nanotubes *in situ* embedded with NiS nanocrystals outperform Pt in dye-sensitized solar cells:

interface improved activity. J Mater Chem A 7:10405–10411. https://doi.org/10.1039/C9TA00649D

Wang B, Huang H, Sun T et al (2020a) Dissolution reconstruction of electron-transfer enhanced hierarchical NiSx-MoO2 nanosponges as a promising industrialized hydrogen evolution catalyst beyond Pt/C. J Colloid Interface Sci 567:339–346. https://doi.org/10.1016/j.jcis.2020.02.027

Wang X-T, Li Y, Zhang X-Q et al (2020) Design and fabrication of NiS/LaFeO3 heterostructures for high efficient photodegradation of organic dyes. Appl Surf Sci 504:144363. https://doi.org/10.1016/j.apsusc.2019.144363

Wild SR, Jones KC (1991) Organic contaminants in wastewaters and sewage sludges: transfer to the environment following disposal. In: Jones KC (ed) Organic contaminants in the environment. Springer, Netherlands, pp 133–158

Wu Z, Xiong Z, Lai B (2022) Metal sulfide-based catalysts in advanced oxidation processes for water decontamination. Environ Funct Mater 1:298–315. https://doi.org/10.1016/j.efmat.2023.01.004

Xi C, Deng P, Miao D et al (2022) Improved charge transfer by binary Ni3S2-NiS2 for boosting the photocatalytic hydrogen generation over g-C3N4. Mater Lett 307:131012. https://doi.org/10.1016/j.matlet.2021.131012

Xue M, Wang X, Li X et al (2021) C3N4 nanosheets loaded with the CuWO4 activated NiS co-catalyst: a stable noble metal-free photocatalyst with dramatic photocatalytic activity for H2 generation and high salinity tolerant. J Photochem Photobiol A Chem 405:112919. https://doi.org/10.1016/j.jphotochem.2020.112919

Yang X, Zhou L, Feng A et al (2014) Synthesis of nickel sulfides of different phases for counter electrodes in dye-sensitized solar cells by a solvothermal method with different solvents. J Mater Res 29:935–941. https://doi.org/10.1557/jmr.2014.74

Yendrapati TP, Ega SP, Abraham BM, Pal U (2022) Hydrothermally decorated robust bimetallic sulfides with heterojunction interfaces for efficient hydrogen generation. Int J Hydrogen Energy 47:40254–40263. https://doi.org/10.1016/j.ijhydene.2022.07.233

Yousfi O, Donnadieu P, Bréchet Y et al (2010) Phase transformations in nickel sulphide: microstructures and mechanisms. Acta Mater 58:3367–3380. https://doi.org/10.1016/j.actamat.2010.02.011

Zhang L, Tian B, Chen F, Zhang J (2012) Nickel sulfide as co-catalyst on nanostructured TiO2 for photocatalytic hydrogen evolution. Int J Hydrogen Energy 37:17060–17067. https://doi.org/10.1016/j.ijhydene.2012.08.120

Zhang Y, Peng Z, Guan S, Fu X (2018a) Data on the synthesis processes optimization of novel β-NiS film modified CdS nanoflowers heterostructure nanocomposite for photocatalytic hydrogen evolution. Data Brief 16:828–842. https://doi.org/10.1016/j.dib.2017.12.016

Zhang Y-X, Li K, Yu Y-X, Zhang W-D (2018b) Carbon nanotubes-modified graphitic carbon nitride photocatalysts with synergistic effect of nickel(II) sulfide and molybdenum(II) disulfide co-catalysts for more efficient H2 evolution. J Colloid Interface Sci 526:374–383. https://doi.org/10.1016/j.jcis.2018.05.003

Zhang X, Tang J, Zhu N et al (2022) Water splitting, pollutant degradation and environmental impact using low-index faceted metal-based nanocrystals. A review. Environ Chem Lett 20:1035–1045. https://doi.org/10.1007/s10311-021-01385-7

Zhao P, Zeng Q, Huang K (2009) Fabrication of β-NiS hollow sphere consisting of nanoflakes via a hydrothermal process. Mater Lett 63:313–315. https://doi.org/10.1016/j.matlet.2008.10.019

Zhao S, Xu J, Li Z et al (2019) Molybdenum disulfide coated nickel-cobalt sulfide with nickel phosphide loading to build hollow core-shell structure for highly efficient photocatalytic hydrogen evolution. J Colloid Interface Sci 555:689–701. https://doi.org/10.1016/j.jcis.2019.08.019

Zhao P, Fu S, Wang X et al (2022) Engineering hierarchically ZnS/NiS/NiS2 hollow porous urchin-like composite towards exceptional lithium storage. J Colloid Interface Sci 624:251–260. https://doi.org/10.1016/j.jcis.2022.05.093

Zheng X, Han X, Zhang Y et al (2019) Controllable synthesis of nickel sulfide nanocatalysts and their phase-dependent performance for overall water splitting. Nanoscale 11:5646–5654. https://doi.org/10.1039/C8NR09902B

Zhou W, Wu X-J, Cao X et al (2013) Ni3S2 nanorods/Ni foam composite electrode with low overpotential for electrocatalytic oxygen evolution. Energy Environ Sci 6:2921. https://doi.org/10.1039/c3ee41572d

Zhu L, Meng Z-D, Ghosh T, Oh W-C (2012) Enhanced photocatalytic efficiency of nanoscale NiS$_2$/TiO$_2$ catalysts synthesized by hydrothermal and sol-gel method. J Korean Ceram Soc 49:135–141. https://doi.org/10.4191/kcers.2012.49.2.135

Zhu C, Jiang Z, Wei W et al (2016) Fabrication of noble-metal-free NiS2/g-C3N4 hybrid photocatalysts with visible light-responsive photocatalytic activities. Res Chem Intermed 42:6483–6499. https://doi.org/10.1007/s11164-016-2475-1

Authors and Affiliations

Anuradha Sharma[1] · Peter R. Makgwane[2,3] · Eric Lichtfouse[4] · Naveen Kumar[1] · Ahmad Hosseini Bandegharaei[5] · Muhammad Tahir[6]

[1] Department of Chemistry, Maharshi Dayanand University, Rohtak 124001, India

[2] Centre for Nanostructures and Advanced Materials (CeNAM), Council for Scientific and Industrial Research (CSIR), Pretoria 0001, South Africa

[3] Department of Chemistry, University of the Western Cape, Private Bag X17, Robert Sobukwe Drive, Bellville 7535, South Africa

[4] European Centre for Research and Education in Geosciences (CEREGE), Aix Marseille, University, 13007 Marseille, France

[5] Faculty of Chemistry, Semnan University, Semnan, Iran

[6] Chemical and Petroleum Engineering Department, UAE University, P.O. Box 15551, Al Ain, United Arab Emirates